

Article

PPAR γ Regulates Triclosan Induced Placental Dysfunction

Jing Li ^{1,2,*}, Xiaojie Quan ^{1,2,†} , Yue Zhang ^{1,2,†}, Ting Yu ¹, Saifei Lei ³, Zhenyao Huang ¹, Qi Wang ¹, Weiyi Song ¹, Xinxin Yang ¹ and Pengfei Xu ^{3,4,*} 

- ¹ School of Public Health, Xuzhou Medical University, 209 Tong-Shan Road, Xuzhou 221002, China; quanxiaojie7@gmail.com (X.Q.); Feb_20th@163.com (Y.Z.); yuting20211213@163.com (T.Y.); huangzhenyao@gmail.com (Z.H.); wangqixzmu2018@163.com (Q.W.); songweiyi798@xzhmu.edu.cn (W.S.); xxyang@xzhmu.edu.cn (X.Y.)
- ² Key Laboratory of Human Genetics and Environmental Medicine, Xuzhou Medical University, Xuzhou 221004, China
- ³ Center for Pharmacogenetics and Department of Pharmaceutical Sciences, University of Pittsburgh, Pittsburgh, PA 15261, USA; sal208@pitt.edu
- ⁴ Beijing Key Laboratory of Gene Resource and Molecular Development, College of Life Sciences, Beijing Normal University, Beijing 100875, China
- * Correspondence: 100002008046@xzhmu.edu.cn (J.L.); pex9@pitt.edu (P.X.)
- † These authors contributed equally to this work.

Abstract: Exposure to the antibacterial agent triclosan (TCS) is associated with abnormal placenta growth and fetal development during pregnancy. Peroxisome proliferator-activated receptor γ (PPAR γ) is crucial in placenta development. However, the mechanism of PPAR γ in placenta injury induced by TCS remains unknown. Herein, we demonstrated that PPAR γ worked as a protector against TCS-induced toxicity. TCS inhibited cell viability, migration, and angiogenesis dose-dependently in HTR-8/SVneo and JEG-3 cells. Furthermore, TCS downregulated expression of PPAR γ and its downstream viability, migration, angiogenesis-related genes *HMOX1*, *ANGPTL4*, *VEGFA*, *MMP-2*, *MMP-9*, and upregulated inflammatory genes *p65*, *IL-6*, *IL-1 β* , and *TNF- α* in vitro and in vivo. Further investigation showed that overexpression or activation (rosiglitazone) alleviated cell viability, migration, angiogenesis inhibition, and inflammatory response caused by TCS, while knockdown or inhibition (GW9662) of PPAR γ had the opposite effect. Moreover, TCS caused placenta dysfunction characterized by the significant decrease in weight and size of the placenta and fetus, while PPAR γ agonist rosiglitazone alleviated this damage in mice. Taken together, our results illustrated that TCS-induced placenta dysfunction, which was mediated by the PPAR γ pathway. Our findings reveal that activation of PPAR γ might be a promising strategy against the adverse effects of TCS exposure on the placenta and fetus.

Keywords: triclosan; PPAR γ ; placenta toxicity; cell migration; angiogenesis; inflammation



Citation: Li, J.; Quan, X.; Zhang, Y.; Yu, T.; Lei, S.; Huang, Z.; Wang, Q.; Song, W.; Yang, X.; Xu, P. PPAR γ Regulates Triclosan Induced Placental Dysfunction. *Cells* **2022**, *11*, 86. <https://doi.org/10.3390/cells11010086>

Academic Editors: Kay-Dietrich Wagner and Nicole Wagner

Received: 9 November 2021

Accepted: 24 December 2021

Published: 28 December 2021

Publisher's Note: MDPI stays neutral with regard to jurisdictional claims in published maps and institutional affiliations.



Copyright: © 2021 by the authors. Licensee MDPI, Basel, Switzerland. This article is an open access article distributed under the terms and conditions of the Creative Commons Attribution (CC BY) license (<https://creativecommons.org/licenses/by/4.0/>).

1. Introduction

Triclosan (TCS) is a synthetic broad-spectrum antimicrobial and exposure mainly occurs in dermal application (soaps, hand sanitizers, toothpaste, cosmetics, antiperspirants, and bedclothes) and oral use of consumer products (water, food products) [1–3]. TCS, as a kind of exogenous biological signal termed Endocrine disruptors (EDCs), can mimic endogenous estrogenic hormones, and interferes with the maintenance of homeostasis and the regulation of developmental processes [4]. Previous epidemiological research demonstrated that TCS has been distinguished in mothers' milk (1–13.6 ng/mL), urine (2.5–107 ng/mL), and cord blood samples [5–7]. In addition, high urinary TCS levels in patients with spontaneous abortion have been reported [8]. A Denmark Odense Child Cohort study stated that median unadjusted urinary TCS was 0.88 ng/mL in pregnant women, and high maternal urinary TCS levels were associated with reduced head and abdominal circumference at birth [9]. Animal experiments suggested that the exposure of

pregnant mice to TCS reduced fetal body weight and viability [8]. TCS has been detected with a concentration of up to 478 ng/L and 1329 ng/g in surface waters and sediment, respectively, in China rivers [10]. Therefore, a further understanding of the toxicity of TCS is important for the inhibition of TCS pollution.

The nuclear receptors, peroxisome proliferator-activated receptors (PPARs) are activated by binding natural ligand-inducible transcription factors such as glitazones [11,12]. PPARs are responsible for metabolism and cell function and have three subtypes including PPAR α , PPAR β/δ , and PPAR γ [13,14]. PPAR γ is highly expressed in reproductive tissues (ovary, testis, uterus, prostate, mammary gland) and the trophoblast labyrinthine zone in rodent placentas and human placentas [15]. PPAR has been suggested to be involved in regulating cell trophoblast proliferation, inflammatory reactions oxidative response, and nutrient transport to mediate placenta development [16–18]. Additionally, research has illustrated that PPAR γ agonists enhanced, while PPAR γ antagonists reduced, proliferative and migratory capabilities of endothelial cells [19]. The vasculature defects were observed in placentas at embryonic GD 9.5 in PPAR γ -null mice [16]. Similar animal experiments implicated embryonic lethality induced by defects in placental vascularization in PPAR γ -null mice [20,21]. The downregulated protein level of PPAR γ was associated with placental disorders [22]. PPAR γ expression levels were also found to be decreased in pregnant mice or zebrafish when exposed to TCS [23,24].

The effect of prenatal TCS exposure on placental toxicity and its role in fetal growth and development are still unclear. Whether the effect of prenatal TCS exposure on placental toxicity is associated with PPAR γ remains to be revealed. Our research aims to clarify the potential character of prenatal TCS exposure on placenta function and its potential mechanism of PPAR γ in the process of placental exposure to TCS.

2. Materials and Methods

2.1. Reagents

TCS (CAS No. 3380-34-5, purity > 98% pure) was obtained from Sigma–Aldrich (Oakville, ON, Canada). DMEM/F12 medium and MEM medium were purchased from KeyGEN BioTECH (Jiangsu, China). RPMI 1640 medium was purchased from GIBCO (Grand Island, N.Y.). Dimethyl sulfoxide (DMSO), fetal bovine serum (FBS), the Cell Counting Kit-8 (CCK-8), and corn oil used was obtained from Vicmed (Busan, Korea) and Macklin (Shanghai, China), respectively, and were analytical grades. The pcDNA-PPAR γ vector and *si*-PPAR γ were purchased from GenePharma (Shanghai, China). Moreover, the rosiglitazone (a specific PPAR γ agonist) and GW9662 (a specific PPAR γ antagonist) were obtained from MedChemExpress (Shanghai, China).

2.2. Cell Culture and Transfection

Thanks to Dr. Xinru Wang from Nanjing Medical University (Nanjing, China) for sending HTR-8/SVneo and JEG-3 cells as a gift to us. HTR-8/SVneo and JEG-3 cells were seeded in DMEM/F12 and MEM medium, respectively, and supplemented with 10% FBS in a 5% CO₂ humidified atmosphere at 37 °C. Based on the manufacturer's instructions, these two cell lines were transfected with small interfering RNA (siRNA) (*si*-PPAR γ ; 20 nM), the control siRNA (*si*-Con; 20 nM), pcDNA-PPAR γ (2 μ g), and pcDNA 3.1 (2 μ g) targeting PPAR γ by Lipofectamine 2000 (Invitrogen, Carlsbad, CA, USA). The medium was replaced after 4 h of cell transfection. After cell transfection for 24 h, they were incubated with triclosan for 24 h. For PPAR γ activation or deactivation, cells were treated with rosiglitazone or GW9662 with 10 μ M for 24 h and pre-treated for 0.5 h before incubating with TCS.

2.3. Animal Treatment

Institute of Cancer Research (ICR) mice, at 10 weeks old and weighing about 30 g, were obtained under a protocol approved by Xuzhou Medical University Animal Center. On day GD 7.5, after the vaginal plug (GD 0.5) was observed in pregnant mice, they were randomly separated into five groups ($n = 8$ per group). All pregnant mice were orally managed with

0, 10, 50, and 100 mg/kg/day TCS and from GD 7.5 to GD 17.5, while control pregnant mice accepted the same volume of corn oil. Firstly, rosiglitazone was dissolved in DMSO, and the ratio of DMSO to corn oil was 1:1000, and pregnant mice were orally administered with rosiglitazone (20 mg/kg/day) together with TCS (100 mg/kg/day). Mice placentas were isolated, put into liquid nitrogen to be quickly frozen and stored at -80°C . According to manufacturers of Xuzhou Medical University Animal Ethics Committee, the entire experiment was performed in a Specified Pathogen-Free (SPF) environment (protocols 201605w025, 25 May 2016 and 202106A237, 25 June 2021).

2.4. Cell Viability Assay

HTR-8/SVneo or JEG-3 cells (5×10^3 cells/well) were seeded into sterile plates of 96 wells in complete medium (DMEM/F12, MEM, 10% FBS). Cells were incubated and cultured with TCS of different concentrations for 24 h. An amount of 10 μL CCK-8 (Vicmed, Busan, Korea) solution was added to each well and incubated for 0.5–4 h at 37°C in a 5% CO_2 atmosphere. The plate was detected at 450 nm on a microplate reader Spark (TECAN, Austria, 30086376).

2.5. Cell Migration Assay

HTR-8/SVneo or JEG-3 cells were grown in 6-well cell plates overnight to obtain approximately 70% confluency. After corresponding treatment, HTR-8/SVneo and JEG-3 cells were starved in 1% serum medium. Scratch wounds were made via a sterile 10 μL pipette tip to obtain three parallel lines. Multiple photographs were taken of the wound using an inverted microscope (KS400; Carl Zeiss Imaging GmbH), and the migration distance was measured by Image J analysis software (National Institutes of Health, v1.8.0). The whole wound closure distance was calculated and the distance of newly covered cells was measured at 0 and 24 h to evaluate migration.

2.6. Tube Formation Assay

Approximately 50 μL Matrigel (10 mg/mL) (BD Biosciences, San Diego, CA, USA) was decked into 96-well plates and allowed to completely solidify at 37°C for 1 h to form a gel. Approximately 5×10^3 /mL HUVECs were suspended in a conditioned medium (the conditioned medium was derived from HTR-8/SVneo and JEG-3 cells and added into the wells of the Matrigel solidified plate. Tube formation in each well was monitored and imaged using an inverted microscope after the plate was incubated at 37°C for 5 h. We repeated the experiment three times independently. Tube branch length was measured with six duplicates per well, while average branch length was taken from three random microscopic fields per well. Each assay was done in triplicate and quantification was conducted with Image J software (National Institutes of Health, v1.8.0).

2.7. Real Time PCR (RT-PCR)

Placental tissues, trophoblast cells, and Trizol (Vicmed, Busan, Korea) were used to isolate total RNA. RNA concentration was detected by Nanodrop 2000 (Thermo, Scientific). The reverse transcription was conducted using SYBR Green qPCR SuperMix and 500 ng of the total RNA was reverse transcribed to cDNA. The quantitative RT-PCR was carried out using SYBR Green Master Mix on a 7500 fast real-time PCR System (Applied Biosystem, Foster, CA, USA) according to the manufacturer's instructions. The mRNA levels were analyzed using the comparative cycle threshold method ($2^{-\Delta\Delta\text{CT}}$), and the relative levels were normalized to the level of GAPDH. The primers were designed by Sangon Biotech (Shanghai, China), and primer sequences were listed in Supplementary Table S1.

2.8. Western Blot Analysis

Total cellular protein was extracted and lysed with RIPA lysis buffer with protease inhibitors (KeyGEN, Nanjing, China) and phosphatase inhibitors (KeyGEN, Nanjing, China). Proteins were separated with 10% SDS-PAGE gels and transferred to PVDF membranes

(Merck Millipore, MA, USA). Membranes were blocked with 5% non-fat milk for 1h and then incubated with primary antibodies of PPAR γ , ANGPTL4, MMP-2, IL-1 β , GAPDH, and tubulin β (Bioword, Beijing, China) overnight at 4 °C. After being washed five times for five minutes, the membranes were incubated with the corresponding secondary antibodies for 1h at room temperature. The protein bands were visualized with an Enhanced Chemiluminescence (ECL) detection kit (Amersham, NJ, USA). The protein bands were analyzed using Image Lab Software (Bio-Rad, CA, USA).

2.9. Statistical Analysis

The above assays were carried out three independent times and all data were carried out by GraphPad Prism 8.3 software (San Diego, CA, USA), and data were exhibited as the mean \pm SEM. The comparison of the data was subjected to a one-way analysis of variance among each independent group. The *t*-test or one-way ANOVA was implemented using the SPSS 19.0 (IBM, Armonk, NY, USA). *p*-value < 0.05 and *p*-value < 0.01 were considered a statistically significant difference and higher significance, respectively.

3. Results

3.1. PPAR γ Is Crucial in Cell Viability Inhibition Induced by TCS

The cell viability of HTR-8/SVneo and JEG-3 cells exposed to TCS at different concentrations was determined by the CCK-8 assay. TCS dose-dependently inhibited cell viability of HTR-8/SVneo and JEG-3 cells, significantly decreasing cell viability at 20 μ M, 30 μ M, or 40 μ M (Figure 1A). Of interest, TCS significantly inhibited PPAR γ mRNA expression levels in those two cell lines especially HTR-8/SVneo cells (Figure 1B).

To investigate whether PPAR γ was involved in the TCS-induced inhibition of cell viability, cell viability was analyzed when PPAR γ was overexpressed and activation (rosiglitazone) or knockdown and inhibition (GW9662), and then exposed to TCS. Rosiglitazone and GW9662 with the concentration of 10 μ M were not toxic in HTR-8/SVneo and JEG-3 cells (Figure S1A). The efficiency of PPAR γ overexpression and knockdown is shown in Figure S1B–D. PPAR γ mRNA and protein expression level was increased when PPAR γ was overexpressed (Figure S1B,C) but decreased after knockdown compared to the control in HTR-8/SVneo and JEG-3 cells (Figure S1B,D). The results exhibited that pcDNA-PPAR γ and rosiglitazone alleviated TCS-elicited cell viability inhibition in HTR-8/SVneo and JEG-3 cells (Figure 1C,D). In contrast, GW9662 and *si*-PPAR γ aggravated the inhibition in these two cell lines (Figure 1C,E). In addition, treatment with rosiglitazone increased the expression of PPAR γ -regulated genes, such as *HMOX1*, *ANGPTL4*, *VEGFA*, *MMP-2*, and *MMP-9*, and decreased the expression of *p65*, *IL-6*, *IL-1 β* , and *TNF- α* in vitro. On the other hand, treatment with GW9662 has an opposite trend (Figure S1E).

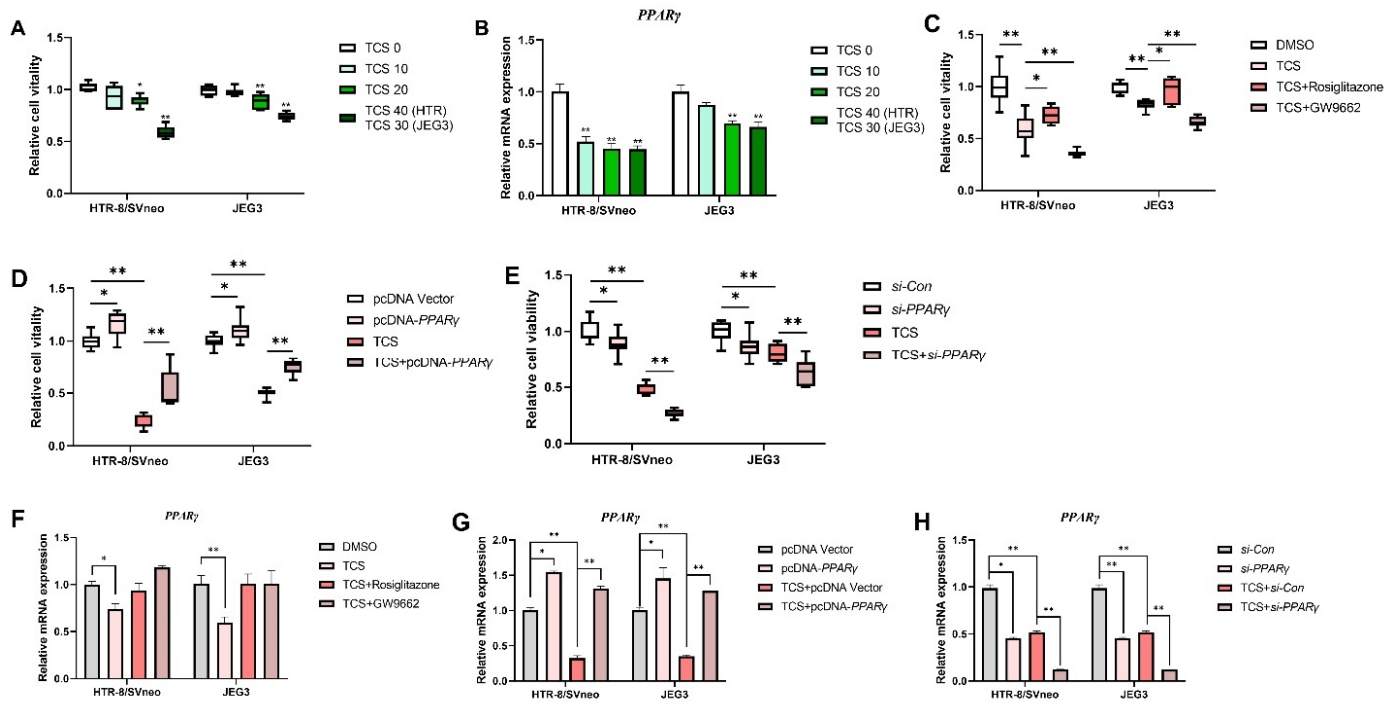


Figure 1. The viability of TCS on HTR-8/SVneo and JEG-3 cells was detected by Cell Counting Kit-8 assay for 24 h. (A) Cell vitality in HTR-8/SVneo and JEG-3 cells exposed to TCS. (B) Expression of PPAR γ was determined by RT-PCR in HTR-8/SVneo and JEG-3 cells exposed to indicated TCS for 24 h. (C) Cell vitality was detected when exposed to TCS (40 μ M for HTR-8/SVneo, 30 μ M for JEG-3) in the absence or presence of rosiglitazone or GW9662 in the two cell lines. PPAR γ was overexpressed (D) and knockdown (E) in the two cell lines and co-treated with TCS in HTR-8/SVneo and JEG-3 cells while cell vitality was analyzed. (F) HTR-8/SVneo and JEG-3 cells exposed to TCS while in the absence or presence of rosiglitazone (10 μ M) and GW9662 (10 μ M). HTR-8/SVneo and JEG-3 cells exposed to TCS during PPAR γ overexpression (G) or knockdown (H). The data are shown as the means \pm S.E.M. * $p < 0.05$; ** $p < 0.01$; compared with the indicated group, $n = 3$.

3.2. PPAR γ Is Involved in TCS-Elicited Impaired Migration

The wound healing assay confirmed that the migration ability of HTR-8/SVneo and JEG-3 cells were inhibited after concentration dependent on exposure to TCS (Figure 2A). To assess the impact of TCS on cell migration influenced by PPAR γ in vitro, the migration assays were conducted in the absence or presence of rosiglitazone or GW9662. Our results in Figure 2B demonstrated that treatment with rosiglitazone significantly increased cell migration, while GW9662 decreased the cell migration compared to the TCS-exposed group in HTR-8/SVneo and JEG-3 cells. PPAR γ displayed overexpression and knockdown in HTR-8/SVneo and JEG-3 cells. Our results indicated that PPAR γ overexpression alleviated the migration inhibition induced by TCS in HTR-8/SVneo and JEG-3 cells (Figure 2C). Moreover, PPAR γ knockdown aggravated the migration inhibition induced by TCS in these two cell lines (Figure 2D).

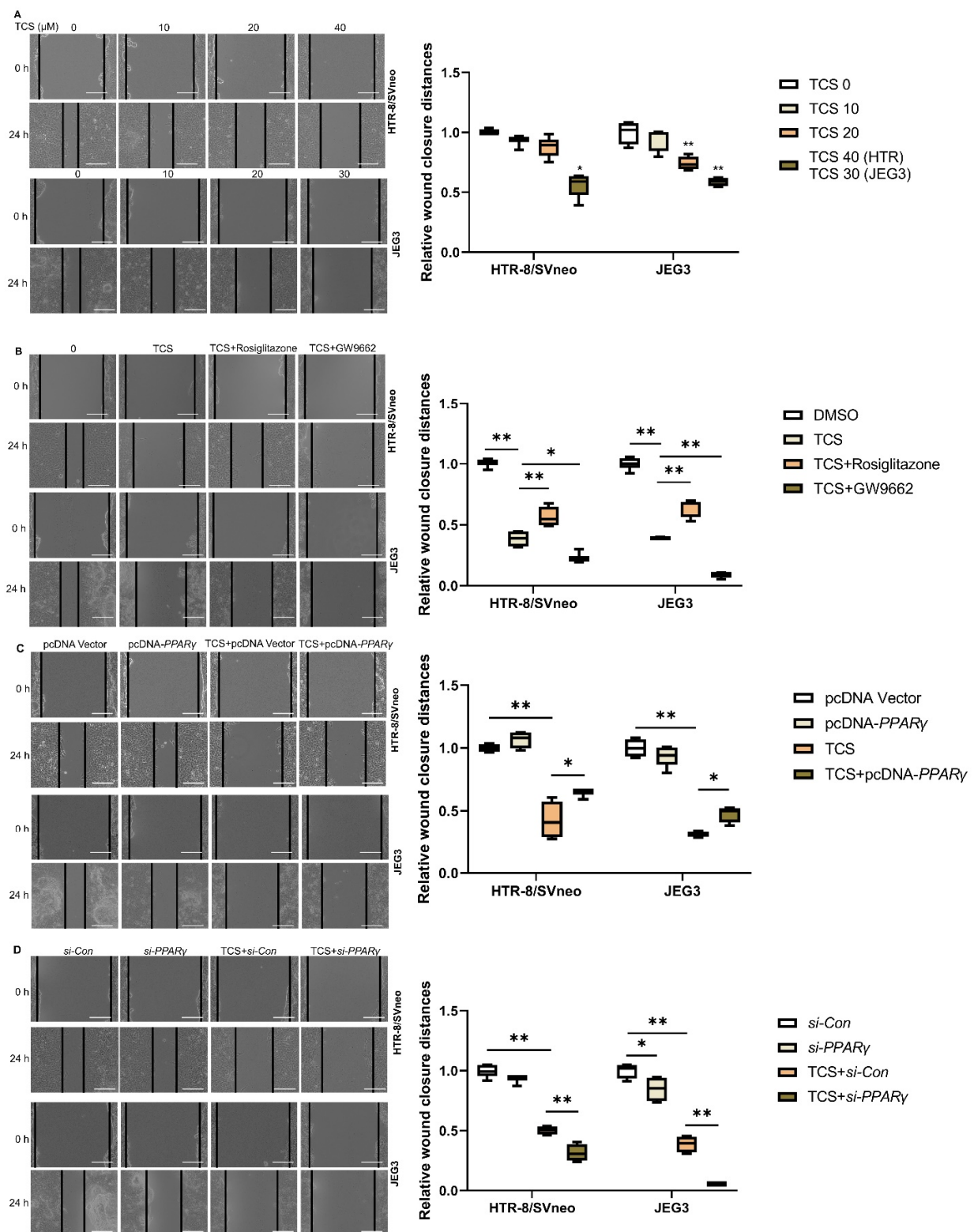


Figure 2. Role of PPAR γ in migration exposed to TCS in vitro. The migration distances were measured after exposure to TCS at 0 h and 24 h. (A) HTR-8/SVneo and JEG-3 cell migration distance was decreased with increasing concentration of TCS. Co-treated with TCS in the absence or presence of rosiglitazone or GW9662 in HTR-8/SVneo and JEG-3 cells (B). The migration distance in response to PPAR overexpression (C) and knockdown (D) when exposed to TCS. Scale bar: 200 μm . The relative wound closure distances are shown on the right. The data are shown as the means \pm S.E.M. * $p < 0.05$; ** $p < 0.01$; compared with the indicated group, $n = 3$.

3.3. PPAR γ Alleviates TCS-Elicited Angiogenesis Inhibition

An angiogenesis assay was implemented to describe the influence of TCS on tube branch length. The HTR8/SVneo and JEG-3 cell lines were treated with different concentrations of TCS. TCS showed significantly decreased tube branch length compared to the control (DMSO) at 30 μ M or 40 μ M in the two cell lines, respectively (Figure 3A). The impact of PPAR γ on TCS-elicited tube branch length is displayed in Figure 3. The existing results illustrated that PPAR γ overexpression or rosiglitazone co-treatment alleviated the inhibition of tube branch length induced by TCS in vitro (Figure 3B,C). In contrast, PPAR γ knockdown or GW9662 co-treatment aggravated the inhibition of tube branch length induced by TCS in HTR8/SVneo and JEG-3 cells (Figure 3B,D).

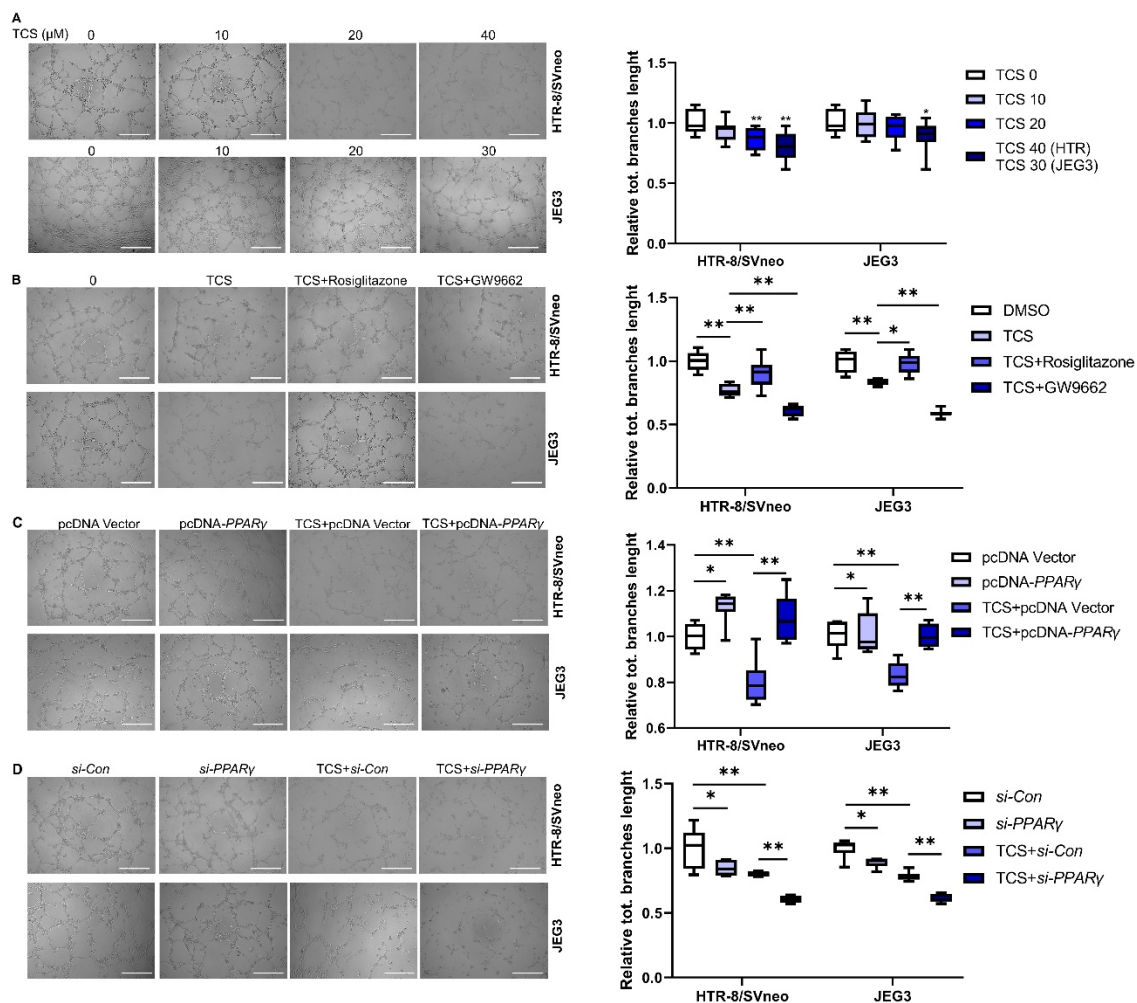


Figure 3. TCS reduced HTR-8/SVneo and JEG-3 cells angiogenesis through PPAR γ pathway. (A) TCS decreased the branch length of HTR-8/SVneo and JEG-3 cells. (B) Co-treated with TCS (40 μ M for HTR-8/SVneo, 30 μ M for JEG-3) in the absence or presence of rosiglitazone and GW9662 in these two cells. (C,D) PPAR γ overexpression alleviated, while (C) PPAR γ knockdown exacerbated. (D) TCS-induced cell angiogenesis inhibition of HTR-8/SVneo and JEG-3 cells. Scale bar: 400 μ m. The data are shown as the means \pm S.E.M. * $p < 0.05$; ** $p < 0.01$; compared with the indicated group, $n = 3$.

3.4. TCS Alters the Expression of PPAR γ Target Genes Associated with Viability, Angiogenesis, and Migration

The *HMOX1*, *ANGPTL4*, *VEGFA*, *MMP-2*, and *MMP-9* genes were determined as the target genes of PPAR γ and play considerable roles in cell viability, angiogenesis, and migration [25–27]. In comparison with the control group, the levels of *HMOX1*, *ANGPTL4*,

VEGFA, *MMP-2*, and *MMP-9* mRNA were significantly decreased in the TCS-exposed group (Figure 4A,B). In addition, the protein levels of *ANGPTL4* and *MMP-2* were significantly decreased in the TCS-exposed groups (Figure 4I,J). We also assessed the influence of *PPAR* γ on the above genes in the absence or presence of TCS. The results revealed that rosiglitazone enhanced the expression of *HMOX1*, *ANGPTL4*, *VEGFA*, *MMP-2*, and *MMP-9* levels, although TCS decreased them in vitro (Figure 4C,D). The *HMOX1*, *ANGPTL4*, *VEGFA*, *MMP-2*, and *MMP-9* mRNA levels were upregulated after overexpression of *PPAR* γ in vitro (Figure 4E,F). In contrast, *PPAR* γ knockdown downregulated the cell viability, angiogenesis, and migration-related genes in HTR-8/SVneo and JEG-3 cells (Figure 4G,H). Therefore, TCS inhibited the *PPAR* γ pathway, leading to the downregulation of *HMOX1*, *ANGPTL4*, *VEGFA*, *MMP-2*, and *MMP-9*.

3.5. TCS Changes Expression Level of *PPAR* γ -Regulated Inflammation Genes

The effect of TCS on *PPAR* γ -regulated inflammatory genes was investigated, and results demonstrated that TCS was able to upregulate genes involved in inflammation such as *p65*, *IL-6*, *IL-1 β* , and *TNF- α* in HTR-8/SVneo and JEG-3 cells (Figure 5A,B). The protein levels of *IL-1 β* were significantly increased in TCS-exposed groups (Figure 4I). However, *PPAR* γ overexpression or rosiglitazone co-treatment significantly alleviated the level of these inflammatory cytokines elicited by TCS in vitro (Figure 5C–F). In addition, *PPAR* γ knockdown or GW9662 co-treatment enhanced the expression levels of those genes elicited by TCS in HTR-8/SVneo and JEG-3 cells (Figure 5C–H). These results emphasized that TCS upregulated inflammatory gene expression through the *PPAR* γ pathway.

3.6. TCS Induces Placenta Dysfunction through *PPAR* γ Pathway in Mice

To reveal the potential toxicity of TCS on the placenta and fetal development, pregnant ICR mice were treated with TCS daily by gavage at doses of 0, 10, 50, and 100 mg/kg/day from gestation day GD7.5 to GD17.5. Uterus, placenta, and fetus were collected for analysis in our study. As the results showed, the size of uterus (Figure 6A), fetus weight (Figure 6B), and placenta (Figure 6C) in TCS-exposed mice were decreased obviously in the 50 and 100 mg/kg/day gavage group compared to the vehicle group, indicating the serious placenta toxicity of TCS. Moreover, rosiglitazone (20 mg/kg/day) administration prevented the decrease of fetus weight (Figure 6B) and placenta diameter (Figure 6C) induced by TCS.

3.7. TCS Alters Expression of *PPAR* γ -Regulated Genes in Mice Placenta

The effects of gestational TCS exposure on viability, migration, angiogenesis, and inflammatory genes in mice placenta were analyzed. As described in Figure 7, placental *Ppar* γ (Figure 7A) and *Ppar* γ -regulated genes *Homx1*, *Angptl4*, *Vegfa*, *Mmp-2*, and *Mmp-9* mRNA levels (Figure 7B) were decreased, while inflammatory genes *p65*, *Il-6*, *Il-1 β* , and *Tnf- α* mRNA levels (Figure 7C) were significantly elevated in TCS-exposed pregnant mice. The protein expression of *ANGPTL4*, *MMP-2*, and *IL-1 β* were consistent with the gene expression trends in the placenta of GD17.5 mice treated with or without TCS (Figure 7D). In addition, treatment with rosiglitazone reversed the *PPAR* γ -regulated viability, migration, angiogenesis, and inflammatory gene expression induced by TCS (Figure 7B,C).

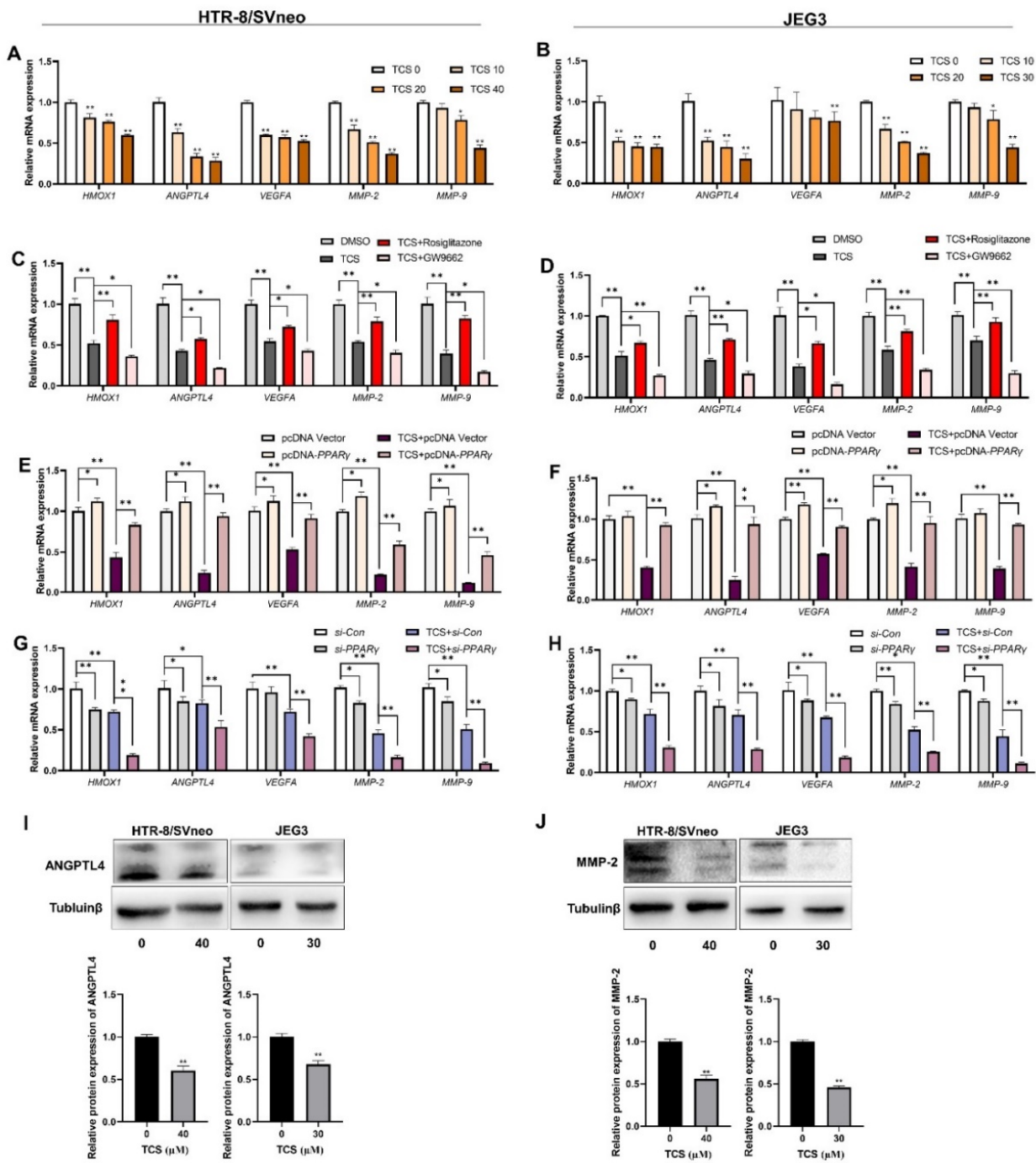


Figure 4. TCS inhibited expression of PPAR γ target genes related to cell vitality, migration, and angiogenesis via PPAR γ pathway in vitro. (A,B) The mRNA expression was analyzed by RT-PCR exposed to the indicated dose of TCS in HTR-8/SVneo and JEG-3 cells. (C,D) HTR-8/SVneo and JEG-3 cells treated with or without rosiglitazone and GW9662 for 24 h in HTR-8/SVneo and JEG-3 cells exposed to TCS (40 μ M for HTR-8/SVneo, 30 μ M for JEG-3). (E–H) PPAR γ was overexpressed (E,F) or displayed knockdown (G,H) and co-treated with TCS in HTR-8/SVneo and JEG-3 cells. (I,J) The protein expression of ANGPTL4 (I) and MMP-2 (J) was analyzed by Western blot in HTR-8/SVneo and JEG-3 cells exposed to TCS. The relative values of protein expression are shown below. The data are shown as the means \pm S.E.M. * $p < 0.05$; ** $p < 0.01$; compared with the indicated group, $n = 3$.

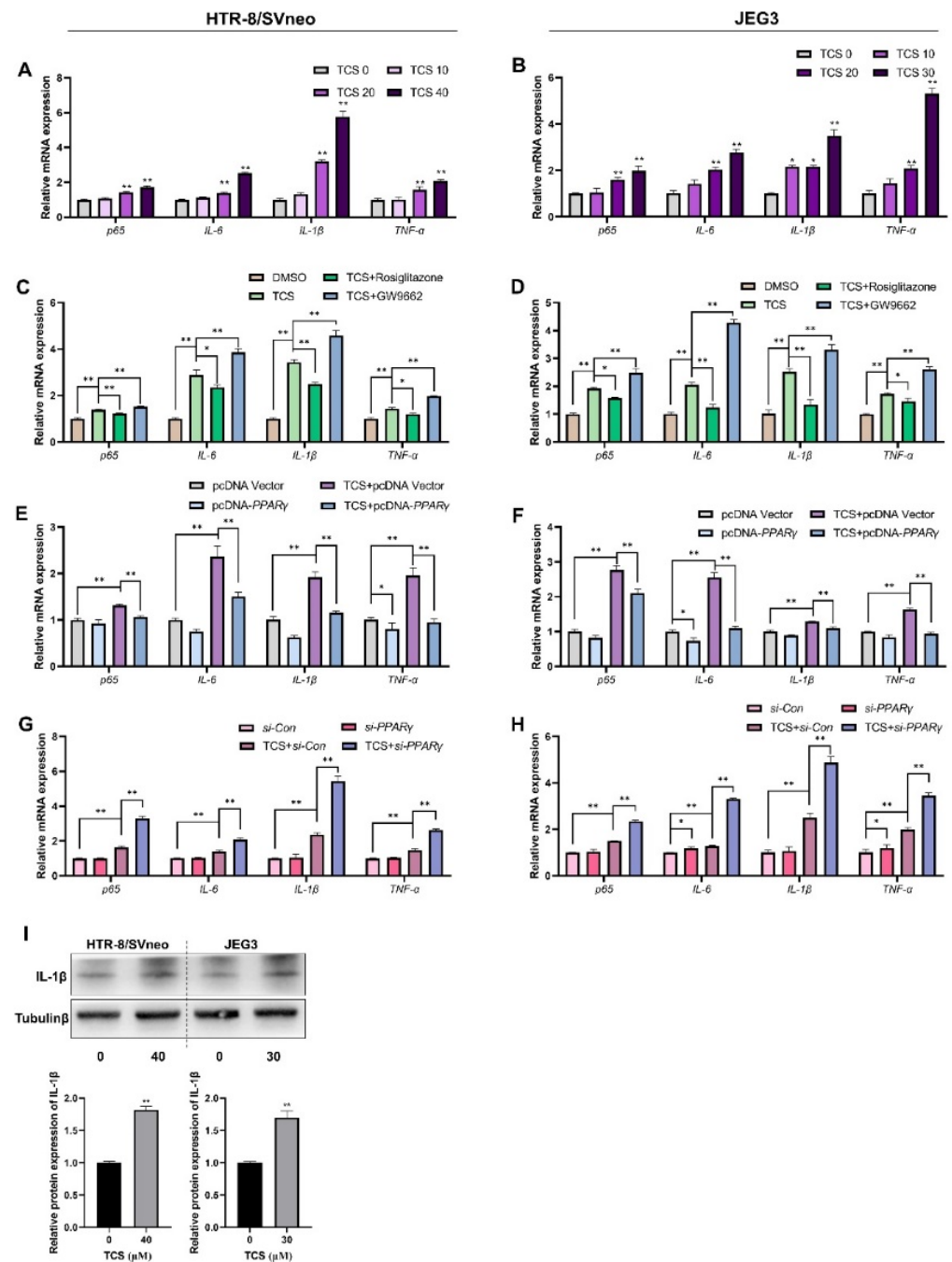


Figure 5. TCS increased expression of PPAR γ -regulated genes related to inflammation through PPAR γ pathway in vitro. (A,B) The mRNA expression level of the inflammatory genes exposed to indicated dose of TCS in HTR-8/SVneo and JEG-3 cells. (C,D) HTR-8/SVneo and JEG-3 cells treated with or without rosiglitazone and GW9662 for 24 h in HTR-8/SVneo and JEG-3 cells co-treated with TCS (40 μ M for HTR-8/SVneo, 30 μ M for JEG-3). (E–H) PPAR γ was overexpressed (E,F) or displayed knockdown (G,H) and co-treated with TCS in HTR-8/SVneo and JEG-3 cells. (I) The protein expression of IL-1 β was analyzed by Western blot in HTR-8/SVneo and JEG-3 cells exposed to TCS. The relative value of protein expression is shown below. The data are shown as the means \pm S.E.M. * $p < 0.05$; ** $p < 0.01$; compared with the indicated group, $n = 3$.

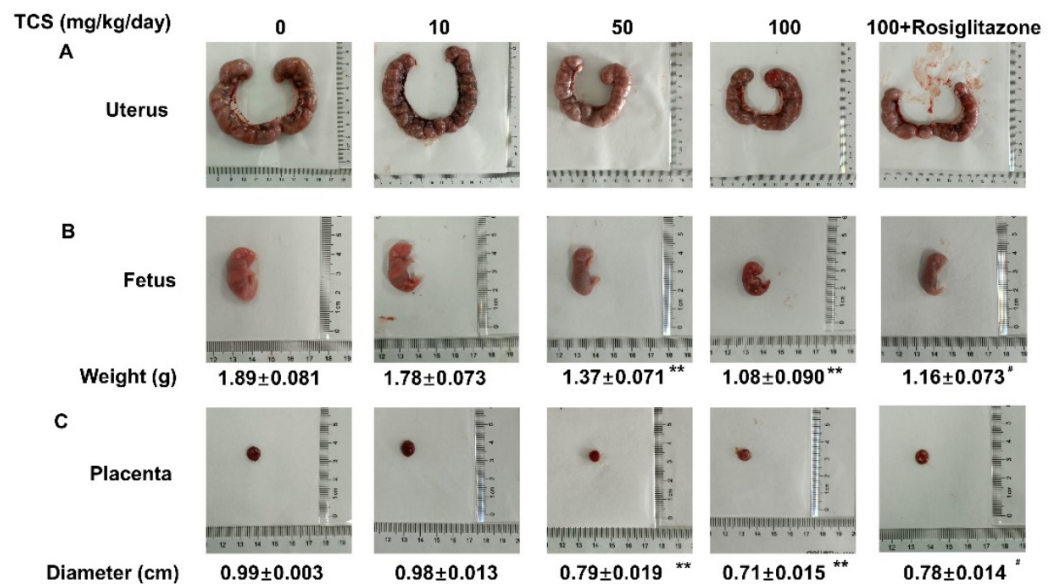


Figure 6. PPAR γ participated in placental and fetal development toxicity of TCS. Representative picture of uterus (A), fetus (B), and placenta (C) of GD17.5 mice exposed to indicated doses of TCS. The data are shown as the means \pm S.E.M; * $p < 0.05$ and ** $p < 0.01$, compared with control group; [#] $p < 0.05$, compared with TCS (100 mg/kg/day) group; $n = 8$.

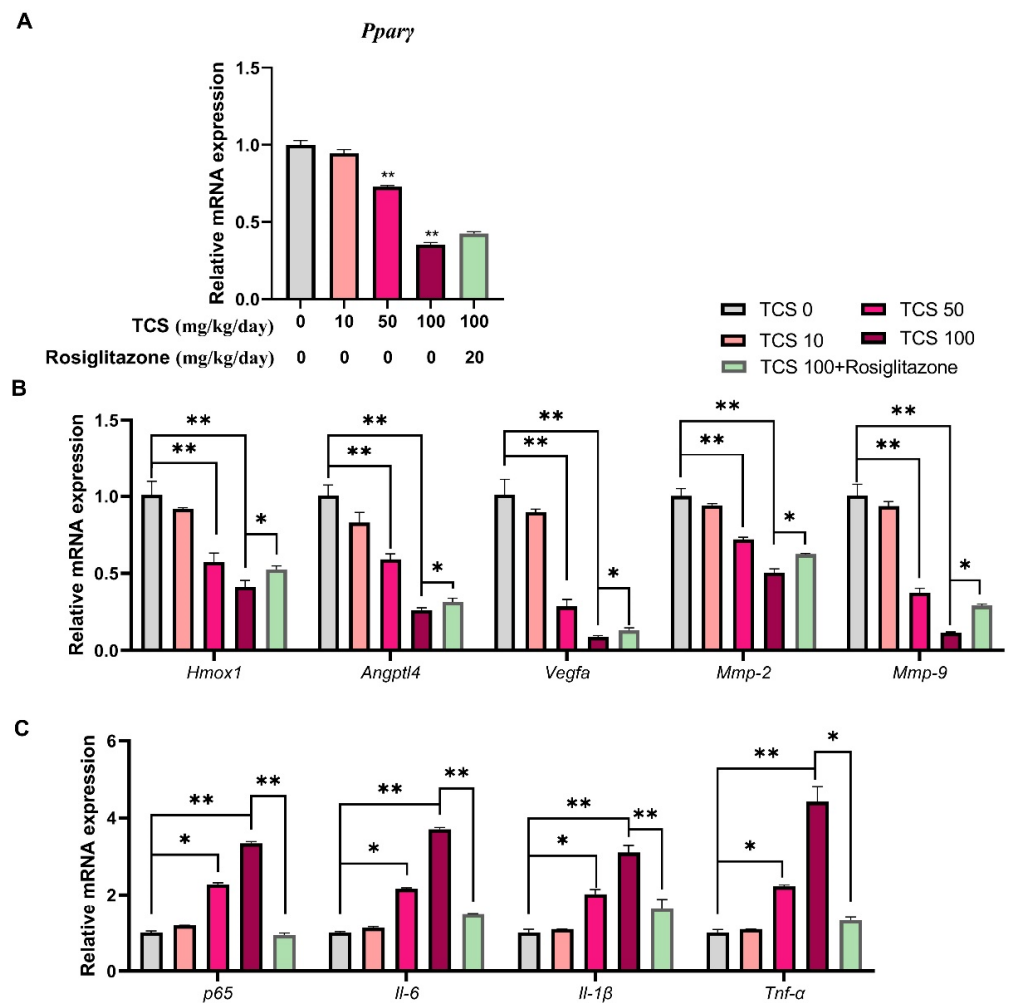


Figure 7. Cont.

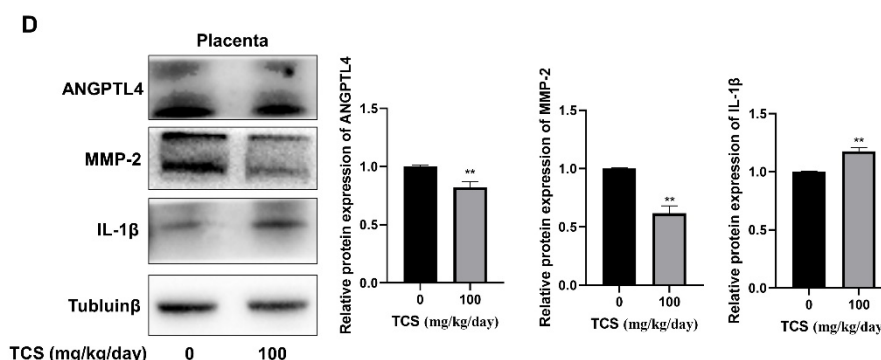


Figure 7. The gene and protein expression of PPAR γ -regulated genes in placentas of gestational mice exposed to TCS. (A) The PPAR γ expression level was detected by RT-PCR in GD17.5 mice placentas. (B,C) The mRNA expression of cell growth, angiogenesis, migration (B), and inflammation (C)-related genes in the placenta of GD17.5 mice treated with indicated doses of TCS and with or without rosiglitazone. (D) The protein expression of ANGPTL4, MMP-2, and IL-1 β were analyzed by Western blot in placenta of GD17.5 mice treated with or without TCS (100 mg/kg/day). The relative values of protein expression are shown on the right. The data are shown as the means \pm S.E.M. * $p < 0.05$; ** $p < 0.01$; compared with the indicated group, $n = 8$.

4. Discussion

In spite of numerous developmental toxicities shown to be triggered by TCS, the mechanism of TCS-elicited severe placental dysfunction has not been well elaborated. Here, our research revealed that TCS dose-dependently inhibited cell growth, migration, angiogenesis in HTR-8/SVneo and JEG-3 cells, and impaired placental development in mice. The mechanism of TCS-induced effects was studied. PPAR γ was partly involved in the toxicity of TCS by regulating placental cell growth, migration, angiogenesis, and inflammatory responses in vitro and in vivo.

Abnormal placental cell proliferation may induce pregnancy complications such as fetal growth retardation, miscarriage, preeclampsia, and macrosomia [28]. Previous studies have verified that TCS had cytotoxic impression, elicited apoptosis, and inhibited cell vitality of human placental trophoblasts [29,30]. Placenta angiogenesis works for placental transport, endocrine, metabolic, and immune function regulation. It is essential for embryogenesis and is involved in the reproductive cycle and wound healing [16]. The intra-placental vascular lesions may result in preeclampsia, fetal growth restriction, or birthweight decrease [31]. Previous research has reported that TCS exposure decreased fetal viability and fetal body weight through placental thrombosis [32]. Some evidence has also demonstrated that TCS stimulated vascular branch disappearance and vascular injury in zebrafish [33]. In our animal research, placental diameter and fetal weight significantly decreased in pregnant mice in the TCS high-dose group. Previous studies have illustrated that the placenta had the greatest bio-accumulation of TCS, and reduced uterine weight and abortion were observed in the TCS (600 mg/kg/day) group in rats [34]. Following TCS exposure, reduction of gravid uterine weight and the occurrence of abortion was observed in pregnant rats [34]. PPAR γ -deficient mice have placental abnormalities and defects in trophoblast differentiation and vascular development [20]. In addition, rosiglitazone increased placental vascularization and trophoblast migration and invasion in villous cytotrophoblast cells (VCT) and placental explants [35]. Our results also proved that PPAR γ was inhibited in the mice placentas after treatment with TCS, and rosiglitazone prevented TCS-induced placenta toxicity by activation of PPAR γ . It will be interesting to know the mechanism by which TCS affects PPAR γ expression. Our results demonstrated that TCS inhibited cell growth, migration, and angiogenesis and influenced placenta development through the PPAR γ pathway in vitro and in vivo.

Vascular endothelial growth factors A (VEGFA) and Heme oxygenase 1 (HO-1) are key modules of the angiogenesis process [36]. Angiopoietin-like protein 4 (ANGPTL4)

is a secretory glycoprotein member of the angiopoietin family, which participates in the regulation of migration and angiogenesis [37,38]. Furthermore, functional studies found that PPAR γ targeted *ANGPTL4* in placental development and angiogenesis, mediating the survival, proliferation, migration, and invasion of HTR8/SVneo cells [39,40]. Our results indicated that PPAR γ activation alleviated the decrease of *HMOX1*, *ANGPTL4*, and *VEGFA* expression caused by TCS. MMPs have been demonstrated to mediate the migration and invasion of trophoblast cells, and *MMP-2* and *MMP-9* expression levels were decreased in preeclamptic placental tissues [41,42]. Similarly, our findings suggested that PPAR γ mediated TCS-induced migration inhibition via *MMP-2* and *MMP-9* expression. In this study, cell growth, migration, and angiogenesis inhibition by TCS was partly ameliorated by PPAR γ elevation or activation. These findings prove that TCS affects cell viability, migration, and angiogenesis through the PPAR γ pathway.

Pregnancy is a process of dynamic inflammatory phases, and the inflammatory state is present almost throughout pregnancy and towards the end [43]. Activation of PPAR γ is reported to suppress inflammation through NF-kappaB and TNF- α [44]. Indeed, pro-inflammatory conditions have been associated with pregnancy complications such as intrauterine growth restriction and preeclampsia [45]. TCS increased the inflammatory response by promoting *TNF- α* and *IL-6* expression in HUVEC [32]. Interestingly, PPAR γ has a critical role in regulating inflammatory cytokines including *TNF- α* and *IL-6*, which were linked to preterm labor, miscarriage, and preeclampsia [22]. Moreover, PPAR- γ has been proved for its anti-inflammatory effects and downregulation of the expression of pro-inflammatory cytokines, such as *IL-6*, *IL-8*, and *TNF- α* , in human gestational tissue [46,47]. Furthermore, activation of PPAR γ by rosiglitazone reversed the LPS-mediated effects on inflammatory cytokine release and proliferation inhibition in HTR-8/SVneo cells [48]. Similarly, we demonstrated that TCS can induce the expression of inflammatory genes in two cell lines. Rosiglitazone or PPAR γ overexpression alleviated PFOS-induced cell growth, migration, angiogenesis inhibition, and the release of inflammatory cytokines in HTR-8/SVneo and JEG-3 cells [49]. Previous studies indicated that decreased PPAR γ expression or the inhibition of PPAR γ activity led to mitochondrial fission, hyperpolarization, and increased oxidative stress [50]. The PPAR γ pathway was one mechanism of triclosan-induced mitochondria-targeted effects, regulating the function of these organelles and the permeability of their membranes [51,52]. Our research showed that PPAR γ activation or overexpression mitigated, while PPAR γ inhibition or silence aggravated the increase of inflammatory gene expression caused by TCS. It is interesting that PPAR γ prevented TCS-induced toxic phenotypes, while treatments with a PPAR γ agonist or antagonist alone had no effects, suggesting some new mechanisms related to PPAR γ can be initiated by TCS, which is worth more future study.

All the results in this study illustrated that TCS caused significant abnormal functions of HTR-8/SVneo and JEG-3 cells, including viability, migration, angiogenesis, and inflammation response. In addition, treatment with rosiglitazone or overexpression of PPAR γ almost completely prevented the abnormal cell function changes in vitro. On the other hand, treatment with GW9662 or *si-PPAR γ* aggravated the toxicity. Similarly, animal studies also indicated that rosiglitazone mitigated the decrease of placental diameter and fetal weight caused by TCS. In addition, curcumin, a natural compound and a modulator of PPAR γ , has been known to have beneficial effects on pregnancy outcomes [53,54]. It will be interesting to know the effect of curcumin or other natural PPAR γ modulators on TCS placental exposure in the future. Our results suggested that TCS placental exposure had adverse effects in vitro and in vivo through the PPAR γ pathway (Figure 8), and activation or increased expression of PPAR γ is a potential strategy to protect against the placenta toxicity induced by TCS.

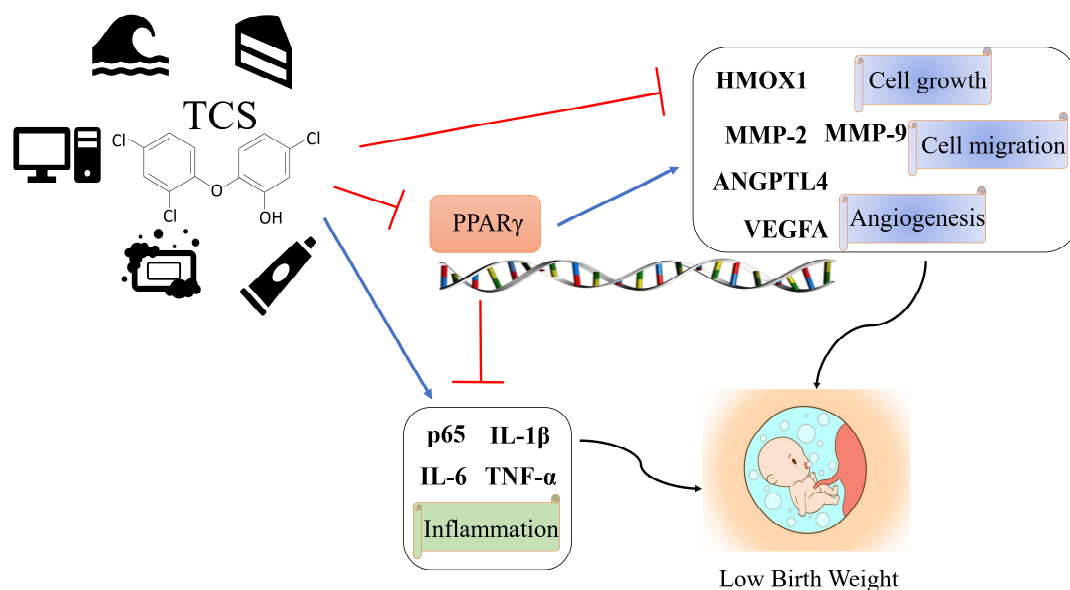


Figure 8. Schematic model depicting TCS-induced placental dysfunction and low birth-weight infants through PPAR γ signaling pathways. TCS inhibited cell growth, angiogenesis, and migration and promoted inflammation of placenta via PPAR γ -regulated genes *HMOX1*, *ANGPTL4*, *VEGFA*, *MMP-2*, *MMP-9*, *p65*, *IL-6*, *IL-1 β* , and *TNF- α* .

Supplementary Materials: The following supporting information can be downloaded at: <https://www.mdpi.com/article/10.3390/cells11010086/s1>, Figure S1: The efficiency of PPAR γ overexpression and knockdown; Table S1: RT-PCR primers.

Author Contributions: Conceptualization, J.L. and P.X.; methodology, X.Q.; formal analysis, J.L. and S.L.; investigation, J.L. and Q.W.; data curation, X.Q., Y.Z. and T.Y.; writing—original draft preparation, X.Q. and Z.H.; writing—review and editing, X.Q., S.L. and P.X.; supervision, J.L., X.Y. and P.X.; project administration, W.S., P.X. and J.L. All authors have read and agreed to the published version of the manuscript.

Funding: This research was funded by the National Natural Science Foundation of China [No. 81703260]; the Science and Technology Department of Jiangsu Province [No. BK20160227]; the China Postdoctoral Science Foundation funded project [No. 2016M601892]; the Priority Academic Program Development of Jiangsu Higher Education Institutions (PAPD), and Jiangsu Overseas Visiting Scholar Program for University Prominent Young and Middle-aged Teachers and Presidents, the Postgraduate Research and Practice Innovation Program of Jiangsu Province (No. KYCX21_2725).

Institutional Review Board Statement: The animal study protocol was approved by the Xuzhou Medical University Animal Ethics Committee, the entire experiment was per-formed in a Specified Pathogen-Free (SPF) environment (protocols 201605w025, 25 May 2016 and 202106A237, 25 June 2021).

Informed Consent Statement: Not applicable.

Data Availability Statement: The data sets generated and/or analyzed during the current study are available from the corresponding author on reasonable request.

Conflicts of Interest: The authors declare no conflict of interest.

References

1. Weatherly, L.M.; Gosse, J.A. Triclosan exposure, transformation, and human health effects. *J. Toxicol. Environ. Health B. Crit. Rev.* **2017**, *20*, 447–469. [[CrossRef](#)]
2. Alfhili, M.A.; Lee, M.-H. Triclosan: An Update on Biochemical and Molecular Mechanisms. *Oxid. Med. Cell Longev.* **2019**, *2019*, 1607304. [[CrossRef](#)]
3. Rodricks, J.V.; Swenberg, J.A.; Borzelleca, J.F.; Maronpot, R.R.; Shipp, A.M. Triclosan: A critical review of the experimental data and development of margins of safety for consumer products. *Crit. Rev. Toxicol.* **2010**, *40*, 422–484. [[CrossRef](#)]

4. Ribeiro, E.; Ladeira, C.; Viegas, S. EDCs Mixtures: A Stealthy Hazard for Human Health? *Toxics* **2017**, *5*, 5. [[CrossRef](#)]
5. Bever, C.S.; Rand, A.A.; Nording, M.; Taft, D.; Kalanetra, K.M.; Mills, D.A.; Breck, M.A.; Smilowitz, J.T.; German, J.B.; Hammock, B.D. Effects of triclosan in breast milk on the infant fecal microbiome. *Chemosphere* **2018**, *203*, 467–473. [[CrossRef](#)]
6. Etzel, T.; Muckle, G.; Arbuckle, T.E.; Fraser, W.D.; Ouellet, E.; Séguin, J.R.; Lanphear, B.; Braun, J.M. Prenatal urinary triclosan concentrations and child neurobehavior. *Environ. Int.* **2018**, *114*, 152–159. [[CrossRef](#)]
7. Ashley-Martin, J.; Dodds, L.; Arbuckle, T.E.; Marshall, J. Prenatal triclosan exposure and cord blood immune system biomarkers. *Int. J. Hyg. Environ. Health* **2016**, *219*, 454–457. [[CrossRef](#)]
8. Wang, X.; Chen, X.; Feng, X.; Chang, F.; Chen, M.; Xia, Y.; Chen, L. Triclosan causes spontaneous abortion accompanied by decline of estrogen sulfotransferase activity in humans and mice. *Sci. Rep.* **2015**, *5*, 18252. [[CrossRef](#)]
9. Lassen, T.H.; Frederiksen, H.; Kyhl, H.B.; Swan, S.H.; Main, K.M.; Andersson, A.-M.; Lind, D.V.; Husby, S.; Wohlfahrt-Veje, C.; Skakkebaek, N.E.; et al. Prenatal Triclosan Exposure and Anthropometric Measures Including Anogenital Distance in Danish Infants. *Environ. Health Perspect.* **2016**, *124*, 1261–1268. [[CrossRef](#)]
10. Zhao, J.-L.; Zhang, Q.-Q.; Chen, F.; Wang, L.; Ying, G.-G.; Liu, Y.-S.; Yang, B.; Zhou, L.-J.; Liu, S.; Su, H.-C.; et al. Evaluation of triclosan and triclocarban at river basin scale using monitoring and modeling tools: Implications for controlling of urban domestic sewage discharge. *Water Res.* **2013**, *47*, 395–405. [[CrossRef](#)]
11. Hong, F.; Xu, P.; Zhai, Y. The Opportunities and Challenges of Peroxisome Proliferator-Activated Receptors Ligands in Clinical Drug Discovery and Development. *Int. J. Mol. Sci.* **2018**, *19*, 2189. [[CrossRef](#)]
12. Xu, P.; Zhai, Y.; Wang, J. The Role of PPAR and Its Cross-Talk with CAR and LXR in Obesity and Atherosclerosis. *Int. J. Mol. Sci.* **2018**, *19*, 1260. [[CrossRef](#)]
13. Hong, F.; Pan, S.; Guo, Y.; Xu, P.; Zhai, Y. PPARs as Nuclear Receptors for Nutrient and Energy Metabolism. *Molecules* **2019**, *24*, 2545. [[CrossRef](#)]
14. Xu, P.; Hong, F.; Wang, J.; Wang, J.; Zhao, X.; Wang, S.; Xue, T.; Xu, J.; Zheng, X.; Zhai, Y. DBZ is a putative PPAR γ agonist that prevents high fat diet-induced obesity, insulin resistance and gut dysbiosis. *Biochim. Biophys. Acta Gen. Subj.* **2017**, *11 Pt A*, 2690–2701. [[CrossRef](#)]
15. Xi, Y.; Zhang, Y.; Zhu, S.; Luo, Y.; Xu, P.; Huang, Z. PPAR-Mediated Toxicology and Applied Pharmacology. *Cells* **2020**, *9*, 200. [[CrossRef](#)]
16. Nadra, K.; Quignodon, L.; Sardella, C.; Joye, E.; Mucciolo, A.; Chrast, R.; Desvergne, B. PPAR γ in placental angiogenesis. *Endocrinology* **2010**, *151*, 4969–4981. [[CrossRef](#)]
17. Fournier, T.; Tsatsaris, V.; Handschuh, K.; Evain-Brion, D. PPARs and the placenta. *Placenta* **2007**, *28*, 65–76. [[CrossRef](#)]
18. Debril, M.B.; Renaud, J.P.; Fajas, L.; Auwerx, J. The pleiotropic functions of peroxisome proliferator-activated receptor gamma. *J. Mol. Med.* **2001**, *79*, 30–47. [[CrossRef](#)]
19. Wagner, N.; Wagner, K.-D. PPARs and Angiogenesis—Implications in Pathology. *Int. J. Mol. Sci.* **2020**, *21*, 5723. [[CrossRef](#)]
20. Barak, Y.; Nelson, M.C.; Ong, E.S.; Jones, Y.Z.; Ruiz-Lozano, P.; Chien, K.R.; Koder, A.; Evans, R.M. PPAR gamma is required for placental, cardiac, and adipose tissue development. *Mol. Cell* **1999**, *4*, 585–595. [[CrossRef](#)]
21. Kubota, N.; Terauchi, Y.; Miki, H.; Tamemoto, H.; Yamauchi, T.; Komeda, K.; Satoh, S.; Nakano, R.; Ishii, C.; Sugiyama, T.; et al. PPAR gamma mediates high-fat diet-induced adipocyte hypertrophy and insulin resistance. *Mol. Cell* **1999**, *4*, 597–609. [[CrossRef](#)]
22. Kadam, L.; Kohan-Ghadr, H.R.; Drewlo, S. The balancing act—PPAR- γ 's roles at the maternal-fetal interface. *Syst. Biol. Reprod. Med.* **2015**, *61*, 65–71. [[CrossRef](#)]
23. Hua, X.; Cao, X.-Y.; Wang, X.-L.; Sun, P.; Chen, L. Exposure of Pregnant Mice to Triclosan Causes Insulin Resistance via Thyroxine Reduction. *Toxicol. Sci.* **2017**, *160*, 150–160. [[CrossRef](#)] [[PubMed](#)]
24. Szychowski, K.A.; Skóra, B.; Wójtowicz, A.K. Triclosan affects the expression of nitric oxide synthases (NOSs), peroxisome proliferator-activated receptor gamma (PPAR γ), and nuclear factor kappa-light-chain-enhancer of activated B cells (NF- κ B) in mouse neocortical neurons in vitro. *Toxicol. Vitro* **2021**, *73*, 105143. [[CrossRef](#)]
25. La Paglia, L.; Listì, A.; Caruso, S.; Amodeo, V.; Passiglia, F.; Bazan, V.; Fanale, D. Potential Role of ANGPTL4 in the Cross Talk between Metabolism and Cancer through PPAR Signaling Pathway. *PPAR Res.* **2017**, *2017*, 8187235. [[CrossRef](#)]
26. Shyu, L.-Y.; Chen, K.-M.; Lu, C.-Y.; Lai, S.-C. Regulation of Proinflammatory Enzymes by Peroxisome Proliferator-Activated Receptor Gamma in Astroglia Infected with *Toxoplasma gondii*. *J. Parasitol.* **2020**, *106*, 564–571. [[CrossRef](#)]
27. Shen, B.; Zhao, C.; Wang, Y.; Peng, Y.; Cheng, J.; Li, Z.; Wu, L.; Jin, M.; Feng, H. Aucubin inhibited lipid accumulation and oxidative stress via Nrf2/HO-1 and AMPK signalling pathways. *J. Cell Mol. Med.* **2019**, *23*, 4063–4075. [[CrossRef](#)]
28. Kelleher, A.M.; DeMayo, F.J.; Spencer, T.E. Uterine Glands: Developmental Biology and Functional Roles in Pregnancy. *Endocr. Rev.* **2019**, *40*, 1424–1445. [[CrossRef](#)]
29. Zhang, N.; Wang, W.; Li, W.; Liu, C.; Chen, Y.; Yang, Q.; Wang, Y.; Sun, K. Inhibition of 11 β -HSD2 expression by triclosan via induction of apoptosis in human placental syncytiotrophoblasts. *J. Clin. Endocrinol. Metab.* **2015**, *100*, E542–E549. [[CrossRef](#)]
30. Honkisz, E.; Zieba-Przybylska, D.; Wojtowicz, A.K. The effect of triclosan on hormone secretion and viability of human choriocarcinoma JEG-3 cells. *Reprod. Toxicol.* **2012**, *34*, 385–392. [[CrossRef](#)]
31. Burton, G.J.; Jauniaux, E. Pathophysiology of placental-derived fetal growth restriction. *Am. J. Obstet. Gynecol.* **2018**, *218*, S745–S761. [[CrossRef](#)]
32. Zhang, M.; Zhu, R.; Zhang, L. Triclosan stimulates human vascular endothelial cell injury via repression of the PI3K/Akt/mTOR axis. *Chemosphere* **2020**, *241*, 125077. [[CrossRef](#)]

33. Zhang, Y.; Liu, M.; Liu, J.; Wang, X.; Wang, C.; Ai, W.; Chen, S.; Wang, H. Combined toxicity of triclosan, 2,4-dichlorophenol and 2,4,6-trichlorophenol to zebrafish (*Danio rerio*). *Environ. Toxicol. Pharmacol.* **2018**, *57*, 9–18. [[CrossRef](#)]
34. Feng, Y.; Zhang, P.; Zhang, Z.; Shi, J.; Jiao, Z.; Shao, B. Endocrine Disrupting Effects of Triclosan on the Placenta in Pregnant Rats. *PLoS ONE* **2016**, *11*, e0154758. [[CrossRef](#)] [[PubMed](#)]
35. Garnier, V.; Traboulsi, W.; Salomon, A.; Brouillet, S.; Fournier, T.; Winkler, C.; Desvergne, B.; Hoffmann, P.; Zhou, Q.-Y.; Congiu, C.; et al. PPAR γ controls pregnancy outcome through activation of EG-VEGF: New insights into the mechanism of placental development. *Am. J. Physiol. Endocrinol. Metab.* **2015**, *309*, E357–E369. [[CrossRef](#)]
36. Shibuya, M. Vascular endothelial growth factor and its receptor system: Physiological functions in angiogenesis and pathological roles in various diseases. *J. Biochem.* **2013**, *153*, 13–19. [[CrossRef](#)]
37. Hato, T.; Tabata, M.; Oike, Y. The role of angiopoietin-like proteins in angiogenesis and metabolism. *Trends Cardiovasc. Med.* **2008**, *18*, 6–14. [[CrossRef](#)]
38. Goh, Y.Y.; Pal, M.; Chong, H.C.; Zhu, P.; Tan, M.J.; Punugu, L.; Tan, C.K.; Huang, R.-L.; Sze, S.K.; Tang, M.B.Y.; et al. Angiopoietin-like 4 interacts with matrix proteins to modulate wound healing. *J. Biol. Chem.* **2010**, *285*, 32999–33009. [[CrossRef](#)]
39. Liu, L.; Zhuang, X.; Jiang, M.; Guan, F.; Fu, Q.; Lin, J. ANGPTL4 mediates the protective role of PPAR γ activators in the pathogenesis of preeclampsia. *Cell Death Dis.* **2017**, *8*, e3054. [[CrossRef](#)]
40. Woeckel, V.J.; Bruedigam, C.; Koedam, M.; Chiba, H.; van der Eerden, B.C.J.; van Leeuwen, J.P.T.M. 1 α ,25-dihydroxyvitamin D3 and rosiglitazone synergistically enhance osteoblast-mediated mineralization. *Gene* **2013**, *512*, 438–443. [[CrossRef](#)]
41. Tian, F.-J.; Qin, C.-M.; Li, X.-C.; Wu, F.; Liu, X.-R.; Xu, W.-M.; Lin, Y. Decreased stathmin-1 expression inhibits trophoblast proliferation and invasion and is associated with recurrent miscarriage. *Am. J. Pathol.* **2015**, *185*, 2709–2721. [[CrossRef](#)]
42. Yang, Y.; Zhang, J.; Gong, Y.; Liu, X.; Bai, Y.; Xu, W.; Zhou, R. Increased expression of prostasin contributes to early-onset severe preeclampsia through inhibiting trophoblast invasion. *J. Perinatol.* **2015**, *35*, 16–22. [[CrossRef](#)]
43. Vannuccini, S.; Clifton, V.L.; Fraser, I.S.; Taylor, H.S.; Critchley, H.; Giudice, L.C.; Petraglia, F. Infertility and reproductive disorders: Impact of hormonal and inflammatory mechanisms on pregnancy outcome. *Hum. Reprod. Update* **2016**, *22*, 104–115. [[CrossRef](#)]
44. Remels, A.H.V.; Langen, R.C.J.; Gosker, H.R.; Russell, A.P.; Spaapen, F.; Voncken, J.W.; Schrauwen, P.; Schols, A.M.W.J. PPAR γ inhibits NF-kappaB-dependent transcriptional activation in skeletal muscle. *Am. J. Physiol. Endocrinol. Metab.* **2009**, *297*, E174–E183. [[CrossRef](#)] [[PubMed](#)]
45. Challis, J.R.; Lockwood, C.J.; Myatt, L.; Norman, J.E.; Strauss, J.F.; Petraglia, F. Inflammation and pregnancy. *Reprod. Sci.* **2009**, *16*, 206–215. [[CrossRef](#)]
46. Jiang, C.; Ting, A.T.; Seed, B. PPAR-gamma agonists inhibit production of monocyte inflammatory cytokines. *Nature* **1998**, *391*, 82–86. [[CrossRef](#)]
47. Lappas, M.; Permezel, M.; Georgiou, H.M.; Rice, G.E. Regulation of proinflammatory cytokines in human gestational tissues by peroxisome proliferator-activated receptor-gamma: Effect of 15-deoxy-Delta(12,14)-PGJ(2) and troglitazone. *J. Clin. Endocrinol. Metab.* **2002**, *87*, 4667–4672. [[CrossRef](#)] [[PubMed](#)]
48. Kadam, L.; Kilburn, B.; Baczyk, D.; Kohan-Ghadr, H.R.; Kingdom, J.; Drewlo, S. Rosiglitazone blocks first trimester in-vitro placental injury caused by NF- κ B-mediated inflammation. *Sci. Rep.* **2019**, *9*, 2018. [[CrossRef](#)] [[PubMed](#)]
49. Li, J.; Quan, X.; Lei, S.; Huang, Z.; Wang, Q.; Xu, P. PFOS Inhibited Normal Functional Development of Placenta Cells via Signaling. *Biomedicines* **2021**, *9*, 276. [[CrossRef](#)] [[PubMed](#)]
50. Yeligar, S.M.; Kang, B.-Y.; Bijli, K.M.; Kleinhenz, J.M.; Murphy, T.C.; Torres, G.; San Martin, A.; Sutliff, R.L.; Hart, C.M. PPAR γ Regulates Mitochondrial Structure and Function and Human Pulmonary Artery Smooth Muscle Cell Proliferation. *Am. J. Respir. Cell Mol. Biol.* **2018**, *58*, 648–657. [[CrossRef](#)] [[PubMed](#)]
51. Teplova, V.V.; Belosludtsev, K.N.; Kruglov, A.G. Mechanism of triclosan toxicity: Mitochondrial dysfunction including complex II inhibition, superoxide release and uncoupling of oxidative phosphorylation. *Toxicol. Lett.* **2017**, *275*, 108–117. [[CrossRef](#)]
52. Belosludtsev, K.N.; Belosludtseva, N.V.; Tenkov, K.S.; Penkov, N.V.; Agafonov, A.V.; Pavlik, L.L.; Yashin, V.A.; Samartsev, V.N.; Dubinin, M.V. Study of the mechanism of permeabilization of lecithin liposomes and rat liver mitochondria by the antimicrobial drug triclosan. *Biochim. Biophys. Acta Biomembr.* **2018**, *1860*, 264–271. [[CrossRef](#)]
53. Tossetta, G.; Fantone, S.; Giannubilo, S.R.; Marzioni, D. The Multifaced Actions of Curcumin in Pregnancy Outcome. *Antioxidants* **2021**, *10*, 126. [[CrossRef](#)]
54. Blanquicett, C.; Kang, B.-Y.; Ritzenthaler, J.D.; Jones, D.P.; Hart, C.M. Oxidative stress modulates PPAR gamma in vascular endothelial cells. *Free Radic. Biol. Med.* **2010**, *48*, 1618–1625. [[CrossRef](#)] [[PubMed](#)]